Journal of Membrane Science 500 (2016) 225–235

Contents lists available at ScienceDirect

Journal of Membrane Science

journal homepage: www.elsevier.com/locate/memsci

Influence of acid pretreatment on ionic conductivity of Nafion® membranes

Rafael Kuwertz*, Carina Kirstein, Thomas Turek, Ulrich Kunz

Institute of Chemical and Electrochemical Process Engineering, Clausthal University of Technology, Leibnizstr. 17, D-38678 Clausthal-Zellerfeld, Germany

ARTICLE INFO

Article history:
Received 2 August 2015
Received in revised form
24 October 2015
Accepted 19 November 2015
Available online 1 December 2015

Keywords:
Nafion® membrane
Fuel cell
Impedance spectroscopy
Ionic conductivity
Acid pretreatment

ABSTRACT

In the present contribution we investigated the influence of the acid pretreatment procedure of Nafion® 117 membranes on the resulting ionic conductivity by using electrochemical impedance spectroscopy. For this purpose, a setup allowing to measure the ionic conductivity at different temperatures, relative humidities, and contact pressures was developed. The state of protonation was determined by the ionic exchange capacity which is a measure of the amount of protonated sulfonic acid groups for the overall ionic exchange ability of the Nafion® membrane. The state of hydration was determined by water uptake and water vapor adsorption while structural observation was conducted by infrared spectroscopy. Additional thermophysical characterization was performed using differential scanning calorimetry. It was found that the pK_a value and the concentration of the used acid for the pretreatment mainly influence the ion exchange capacity, whereas the temperature during pretreatment mainly influences the water uptake. The combination of high values for temperature, relative humidity and contact pressure leads to enhanced ionic conductivity of Nafion® membranes with a maximum value of 85.2 mS cm^{-1} for the membrane pretreated with HCl.

1. Introduction

Polymer electrolyte membrane fuel cells (PEMFCs) and membrane electrolyzers have become very promising technologies for energy conversion and storage as well as energy-efficient synthesis of important chemicals such as chlorine [1,2]. The performance of a PEMFC/electrolyzer substantially depends on the water management which is controlled by humidification of the membrane [3]. The ionic conductivity of the most frequently used Nafion® membrane [4–7] is determined by temperature and water content, i.e. the ratio of water and sulfonic acid groups. Furthermore, the applied pretreatment procedure strongly influences the water content [8] and hence the resulting ionic conductivity of the membrane. During pretreatment, the type of proton-donating acid, the acid concentration as well as the applied temperature governs the ionic conductivity.

Nafion® consists of a perfluorinated backbone (PTFE) with perfluorovinyl ether side chains terminated with sulfonic acid groups ($-SO_3H$). The transport of ions in this material is described with the network-cluster model by Gierke et al. [9,10] according to which the membrane is a mixture of two phases with hydrophobic (PTFE) and hydrophilic ($-SO_3H$) domains. The hydrophilic domains are clusters established within the hydrated membrane containing the sulfonic acid groups, water and protons. These clusters expand with increasing water content and are connected by channels to assure the proton conductivity. The charge transport in the membrane is described by a proton-hopping (Grotthuss) and/or a vehicle mechanism [11,12]. The Grotthuss mechanism describes the transport of the charge at low water contents with hydronium (H_3O^+) ions being formed by one hydrated sulfonic acid group followed by charge transfer to the next sulfonic acid group. The vehicle mechanism in contrast describes the transport of the hydronium ions through diffusion caused by electroosmotic drag with the formation of Zundel ($H_5O_2^+$) and Eigen ($H_9O_4^+$) ions. The temperature dependency of the conductivity can be described by an Arrhenius approach. A further proton conducting mechanism was reported by di Noto et al. and Giffin et al. [13,14] which describes the conduction of protons between clusters in embedded “delocalized bodies (DB)”. The charge (H^+) is considered to be delocalized in DB which represents a volume of bulk membrane consisting of both the hydrophobic and hydrophilic domains. Within the DB the proton exchange is fast whereas the proton transfer between two DBs is slower representing the rate-determining step. Furthermore, the proton conduction is facilitated by the polymer backbone dynamics which is the PTFE backbone in the case of Nafion®. Giffin et al. [14] correlate the additional contribution of the polymer dynamics with a Vogel-Tamman-Furcher behavior (VTF) which takes the viscosity of the polymer

---

* Corresponding author.
E-mail address: kuwertz@icvt.tu-clausthal.de (R. Kuwertz).

http://dx.doi.org/10.1016/j.memsci.2015.11.022
0376-7388/© 2015 Elsevier B.V. All rights reserved.

also into account. In constrast to the log-linear temperature dependency described by Arrhenius, the VTF approach is non-linear which results in different activiation energies. The water uptake of the membrane varies depending on whether the membrane is exposed to liquid or to vaporous water. This is described by the well-known Schroeder's paradox [15,16] depicting the alteration in swelling behavior of gelatin facing either liquid or vaporous water. Several research groups have investigated the influence of water vapor and liquid water on the overall water content of Nafion® membranes [17–24]. Transport parameters such as the diffusion coefficient of water through Nafion® and the proton conductivity as a function of the water content are the most interesting data resulting from these considerations. Electrochemical impedance spectroscopy (EIS) became in this context the most promising technique to measure the proton conductivity. Another technique used by di Noto et al. and Giffin et al. [13,14,25] is the so-called broadband electric spectroscopy (BES) which enables to differentiate between bulk and interfacial conductivity of polymer membranes and polymer membranes incorporating anorganic fillers. Zawodzinski et al. investigated the water uptake of Nafion® membrane at different operational parameters like temperature and relative humidity [17,26]. These authors were able to show that the pretreatment procedure is decisive for the resulting water uptake capacity. Many research groups apply hydrogen peroxide in order to remove organic impurities. Furthermore, several scavenging processes with deionized water are applied during the pretreatment procedure. The most important step is the protonation with an acid. Table 1 summarizes the applied pretreatment procedures described in literature. The pretreatment procedures differ with respect to duration, temperature, type of acid, and acid concentration.

To the best of our knowledge there is no systematic study of the influence of the acid pretreatment on the resulting ionic conductivity of Nafion® membranes. Therefore, we investigated in this contribution the influence of acid type and concentration as key pretreatment parameters for the resulting ionic conductivity of Nafion®. Furthermore, operational parameters like relative humidity, temperature and contact pressure were systematically varied. For this purpose an experimental setup allowing the determination of the ionic conductivity by EIS at relative humidities ranging from 20 to 100%rH, temperatures between 20 and 80 °C and contact pressures up to 1000 kPa was designed. Additional characterization was carried out by differential scanning calorimetry. The state of hydration was determined by water uptake and water vapor adsorption while structural observation was performed by infrared spectroscopy. Furthermore, the ion-exchange capacity was measured to estimate the amount of protonated sulfonic acid groups in the Nafion® membrane.

Table 1
Pretreatment procedures for Nafion® membranes.

Acid	Concentration	Temperature	Time	Ref.
H_2SO_4	0.5 M	20 °C, 70–80 °C, 100 °C	20 min, 60 min, 48 h	[17,27–32]
H_2SO_4	1.0 M	100 °C	45 min,60 min	[33–37]
HNO_3	–	100 °C	–	[21]
HNO_3	70%	100 °C	5 h	[38]
HNO_3	Conc.	100 °C	–	[39]
HNO_3	2 M	100 °C	2 h	[40]
HNO_3	0.1 M	100 °C	1 h	[41]
HCl	2 M	20 °C, 100 °C	30 min,3 h	[42,43]
H_3PO_4	85%	150 °C	12 h	[44]

2. Experimental and methods

2.1. Pretreatment of Nafion® membranes

Nafion® 117 membranes in the H^+ form as delivered by DuPont were cut into six circular pieces with a diameter of 50 mm before pretreatment. For each pretreatment step, six membranes were immersed in 0.5 L stirred liquid. The pretreatment procedure which is summarized in Table 2 consisted of a first step in deionized water, followed by a purification step with hydrogen peroxide. Subsequently, three washing steps in deionized water, the acid treatment and afterwards three additional washing steps in deionized water were applied. The temperature during all steps was set to 80 °C while the duration of each step was one hour. Between the steps the membrane was rinsed with deionized water. For all acids (HNO_3, HCl, H_2SO_4, H_3PO_4), 0.1 M and 1 M solutions were applied. The acids were chosen with respect to the amount of protons and their dissociation behavior. All other parameters of the procedure were kept constant. After pretreatment the membranes were stored in deionized water at room temperature. For comparison the untreated membrane was also investigated.

2.2. Characterization techniques

Differential scanning calorimetry (DSC 820, Mettler-Toledo) measurements were used to determine endothermic or exothermic effects during thermal treatment. The probes were heated from 25 °C to 200 °C with a heating rate of 10 K min^{-1} under nitrogen atmosphere (50 mL min^{-1}). To investigate changes in the chemical structure and in particular to sulfonic acid groups, Fourier transformed infrared spectra (FT-IR) were recorded with a stepscan FT-IR spectrometer (Portmann Instruments AG) from 4000 to 500 cm^{-1}.

The ion exchange capacity (IEC) is expressed as the ratio of moles of sulfonic acid groups per gram of dried membrane (m_{probe}) in meq g^{-1}. One piece (ca. 150 mg) of the respective pretreated membrane was stored for 48 h in 50 mL 0.1 mol L^{-1} NaCl solution (V_{NaCl}) to exchange protons with sodium ions. Afterwards 10 mL of the solution ($V_{NaCl,probe}$) were titrated with 0.001 mol L^{-1} NaOH solution ($V^*_{NaOH,probe}$, c_{NaOH}) until neutralization, controlled with a pH probe (pH electrode, WinLab®). The IEC is calculated using Eq. (1) with F being the titer factor of the NaOH solution.

$$\mathrm{IEC}\left(meq\ g^{-1}\right)=\frac{\left(V^*_{NaOH,probe}\right)}{m_{probe}}\cdot c_{NaOH}\cdot\frac{V_{NaCl}}{V_{NaCl,probe}}\cdot F \tag{1}$$

The water uptake (WU) of the membranes was determined by two techniques. First, the uptake of liquid water was investigated. For this purpose, the samples were equilibrated for 48 h at different temperatures (25, 40, 60, 90 °C) in deionized water (one membrane with ca. 650 mg in 200 mL water). Then the excess water on the surface of the samples was removed with a paper tissue and the membranes were weighted (m_{wet}). Afterwards, the membranes were dried in a furnance at 90 °C until constant weight (m_{dry}) was achieved. The water uptake was then calculated

Table 2
Pretreatment procedure for Nafion® 117 membranes.

Time	Concentration	Reagent	Temperature
60 min		Deionized H_2O	80 °C
60 min	3 wt%	H_2O_2	80 °C
3 × 60 min		Deionized H_2O	80 °C
60 min	1 or 0.1 M	Acid	80 °C
3 × 60 min		Deionized H_2O	80 °C

using Eq. (2) [45].

$$WU = \frac{m_{wet} - m_{dry}}{m_{dry}} \cdot 100\ \% \tag{2}$$

Second, the water uptake was determined using a sorption system (ASAP 2020, Micromeritics) with water vapor as sorption gas. The samples were in a first step degassed to remove surface impurities (evacuation at 26.7 Pa and heating to 80 °C for 120 min). Afterwards, the relative pressure of water vapor was increased isothermally from 0 to 1 at 10 °C and the amount of adsorbed water vapor was measured.

2.3. Experimental setup

The experimental setup was inspired by the design of di Noto et al. [46] allowing individual variation of operating parameters such as temperature (20–80 °C), relative humidity (20–100%rH), contact pressure (0–1000 kPa) during measurement of the ionic conductivity of Nafion® using EIS. The measurement cell consisted of a double jacket cylinder made of stainless steel. The cell temperature was controlled by a thermostat (Ecoline E200, Lauda) allowing for adjustment in the range of 25–80 °C. The complete setup of the cell is depicted in Fig. 1. Temperature sensor, humidity sensor, load cell (LCMFD-2KN, Newport Electronics) as well as inlet and outlet for the humidified gas are integrated by Swagelok connectors at the top of the apparatus. A combined sensor (DKRF410-XXS, Driesen+Kern) was used for temperature and humidity measurement. The membrane was clamped between two circular frames made of stainless steel with an inner diameter of 30 mm. Matching PTFE foils were used as insulators. Two 5 mm thick electrodes made of platinated (via CVD coating from Doduco) CrNi-steel sinter metal (SIKA-R10, GKN Sinter Metals Filters) with a diameter of 28.5 mm were used for conductivity measurements. The porous sinter metal electrodes (pore radius approximately 20 μm) are permeable for the humidified gas. Therefore, an equilibration of the membrane under the adjusted measurement conditions was achieved. The force on the electrodes was adjusted by opposed running threads which are connected by bevel gears. These are regulated by a handle on top of the measurement cell. The contact pressure was then calculated by taking into account the applied force and the electrode area.

The measurement cell was integrated into a plant (Fig. 2) consisting of humidifier unit, potentiostat (Reference 3000, Gamry Instruments), and an electrical measurement, regulation and control (EMR) unit. The humidifier unit consisted of a double jacket glass cylinder filled with ca. 1000 mL deionized water. The humidifier was heated through the jacket by a thermostat (CC-K6, Huber) equipped with an external temperature sensor (HSRTD-3–100-A, Omega) inside the wash bottle. The outlet of the humidifier was linked via a heat exchanger to the measurement cell to prevent condensation of water. Furthermore, the heat exchanger was connected to the same thermostat of the cell. The relative humidity was adjusted through the temperature differences between humidifier and cell. Oxygen was used as carrier gas passing the humidifier. The flow rate was adjusted with a needle valve at 200 mL min^{-1} and monitored with a flow meter (Uniflux, VAF Fluidtechnik).

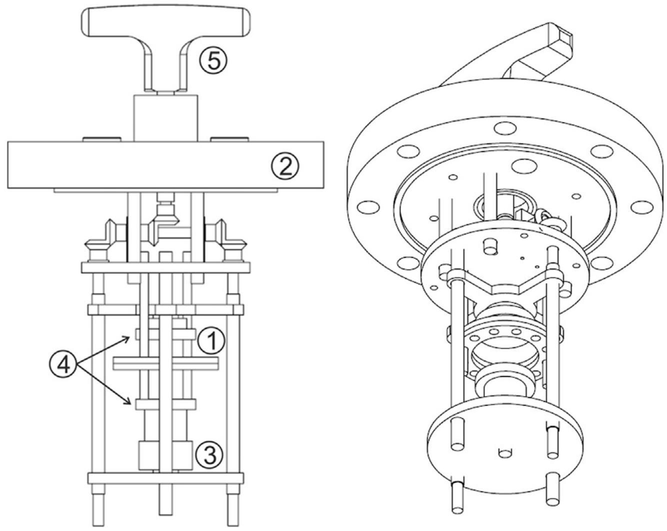

Fig. 1. Measurement cell (1 membrane clamped into frames; 2 top; 3 load cell; 4 sinter metal electrodes; 5 handle to adjust contact pressure).

The EMR unit consisted of temperature, humidity, and load cell sensors which were connected via an analog input module (NI9215, National Instruments) and a computer. The measurement values were recorded via LabVIEW (National Instruments).

The measurement sequence consisted of several steps. First, the membrane was clamped between the stainless steel frames and dried overnight in a furnace at the temperature which was afterwards applied in the measurement cell. Second, initial conditions in the measurement cell were established by dehumidification with silica gel (ca. 6%rH). Afterwards, the dried membrane was mounted in the cell and the operating conditions (humidity and temperature) were adjusted. An impedance spectrum was recorded until equilibrium of the measurement conditions was achieved (after ca. 2–3 h). Additional impedance spectra were taken every 30 min until the resistance of the membrane was constant. After reaching equilibrium, impedance spectra were taken at different contact pressures, which were increased from 100 kPa to 1000 kPa in steps of 100 kPa and decreased in the reverse order. Measurements were conducted at humidities of 25, 40, 60, 80, and 100%rH as well as temperatures of 25, 40, 60, and 80 °C.

2.4. Electrochemical impedance spectroscopy

Electrochemical impedance spectroscopy (EIS) was used to determine the impedance of the membrane and hence to calculate the ionic conductivity of the membrane. As test sequence the HybridEIS script (Gamry Framework, Gamry instruments) with the following configuration was used:

1. DC current = 0 A
2. amplitude = 5 mV
3. frequence range = 100 Hz – 1 MHz; 10 points per decade
4. electrode area = 6.379 cm^2.

The internal resistance of the measurement cell R_{cell} was obtained at each contact pressure value.

The analysis of the EIS spectra was carried out with the Echem Analyst software (Gamry Instruments) using the simplex method. The spectra were fitted with an equivalent circuit diagram developed for fuel cells by Lvovich (Fig. 3) [47]. It consists of four parts which represent the two sinter metal electrodes, the cable connections and the membrane. Each electrode can be described with a constant phase element (CPE_{E1}, CPE_{E2}) connected in parallel with an ohmic resistance (R_{E1}, R_{E2}). The cable connections are described with an inductor (I_0) and cell resistances with an ohmic resistance (R_M) connected in series. To determine the pure membrane resistance (R_{mem}) the measured cell resistance (R_{cell}) is subtracted from R_M.

To calculate the conductivity (σ_{mem}) of the membrane Eq. (3) was used with a_{mem} being the membrane area of 6.379 cm^2 and d_{mem} the thickness of the membrane:

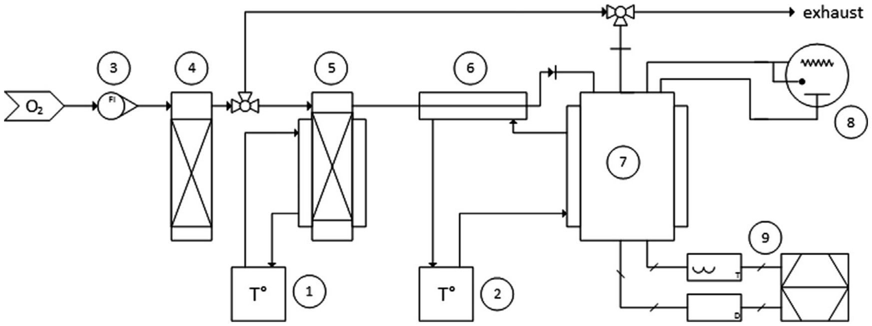

Fig. 2. Flow chart of the experimental setup (1,2 thermostats; 3 flow meter; 4 dehumidifier; 5 humidifier unit; 6 heat exchanger; 7 measurement cell; 8 potentiostat; 9 EMR unit).

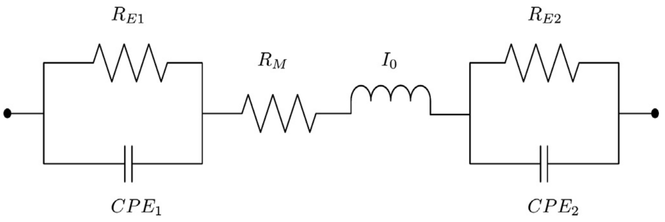

Fig. 3. Equivalent circuit diagram for fitting the EIS spectra.

$$\sigma_{mem} = \frac{d_{mem}}{R_{mem} \cdot a_{mem}} \tag{3}$$

The thickness of the membrane has a great impact on the conductivity. As reported by Weber et al. the thickness of Nafion® 117 varies with the water content (λ) in a range from 178 to 224 μm (26%) [48,49]. Therefore, the reported membrane model (see Appendix) from Weber et al. was used to calculate the membrane thickness for all investigated humidity and temperature combinations.

3. Results and discussion

3.1. Characterization of membranes

3.1.1. Ionic exchange capacity

In Fig. 4 the IEC of the differently pretreated membranes is depicted relative to the value of the untreated membrane ($0.705\ mmol_{SO_3H} g^{-1}_{Nafion}$) for two different acid concentrations (0.1 M and 1 M). Pretreatment with the diluted acid (0.1 M, left columns) results in an enhanced IEC for sulfuric (+2%) and hydrochloric acid (+12%). In contrast, treatment with nitric (−21%) and phosphoric acid (−25%) deteriorates the IEC of Nafion® significantly.

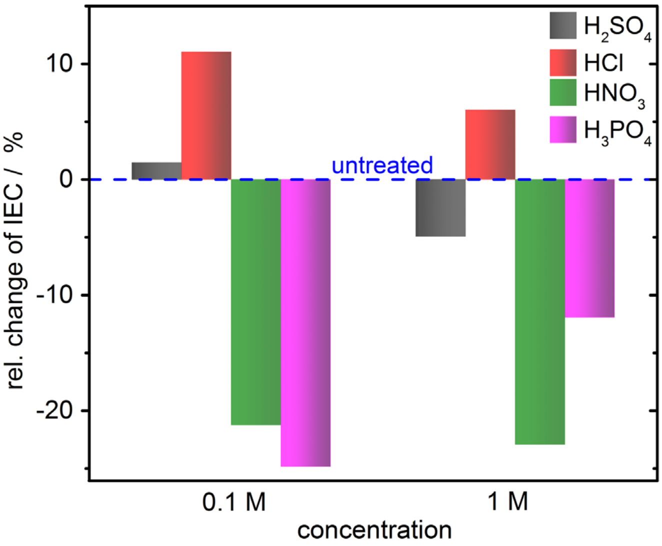

Fig. 4. Ion-exchange capacity for different pretreated membranes as relative change to untreated membrane ($0\% \triangleq 0.705\,mmol_{SO_3H} g^{-1}_{Nafion}$).

Increasing the acid concentration from 0.1 M to 1 M (right columns) results in a decline of the IEC, except for 1 M H_3PO_4. For example, the IEC of the membrane pretreated with 1 M sulfuric acid (-5%) decreases by 7% in comparison to the membrane pretreated with 0.1 M H_2SO_4. Only treatment with 1 M HCl has a positive effect on the IEC (+6%) in comparison to the untreated membrane. On the other hand, the IEC of the membrane pretreated with 1 M phosphoric acid (−12%) shows an improvement of 13% in comparison to 0.1 M H_3PO_4.

The pK_a values (Table 3) show that HCl is a stronger acid than the sulfonic acid in Nafion®, hence a complete protonation is possible. On the other hand, the pK_a values of H_2SO_4 and the sulfonic acid in Nafion® are similar, thus the influence of acid pretreatment is rather weak. For acids with a lower pK_a value than the sulfonic acid group such as HNO_3 and H_3PO_4, the protonation is incomplete, hence leading to a lower IEC compared to the untreated membrane.

3.1.2. Water uptake

The results of the liquid water uptake (WU) are depicted in Fig. 5a, and b for the chosen acids and acid concentrations. The membranes pretreated with 0.1 M acids (Fig. 5a) exhibit relatively similar values for the WU at 25 and 60 °C. However, a significant increase of WU is observable at a measurement temperature of 90 °C. In contrast, the untreated membrane exhibits a linear increase of the WU at rising temperature reaching the same WU as the pretreated membranes (41.5%) at 90 °C. In Fig. 5b the WU of the membranes pretreated with 1 M acids is depicted. Similar

Table 3
pK_a values and degrees of dissociation α of H_2SO_4, H_3PO_4, HNO_3, HCl [50] and Nafion® (R-SO_3H) [51].

	pK_a values	Degree of dissociation α	
		0.1 M	1 M
$H_2SO_4 + H_2O \rightarrow HSO_4^- + H_3O^+$	−3.00	1	0.999
$HSO_4^- + H_2O \rightarrow SO_4^{2-} + H_3O^+$	1.96	0.281	0.099
$H_3PO_4 + H_2O \rightarrow H_2PO_4^- + H_3O^+$	2.16	0.231	0.080
$H_2PO_4^- + H_2O \rightarrow HPO_4^{2-} + H_3O^+$	7.21	$0.785 \cdot 10^{-3}$	$0.248 \cdot 10^{-3}$
$HPO_4^{2-} + H_2O \rightarrow PO_4^{3-} + H_3O^+$	12.32	$0.219 \cdot 10^{-5}$	$0.692 \cdot 10^{-6}$
$HNO_3 + H_2O \rightarrow NO_3^- + H_3O^+$	−1.37	0.996	0.961
$HCl + H_2O \rightarrow Cl^- + H_3O^+$	−7.00	1	1
$R - SO_3H + H_2O \rightarrow R - SO_3^- + H_3O^+$	−3.09	1	0.999

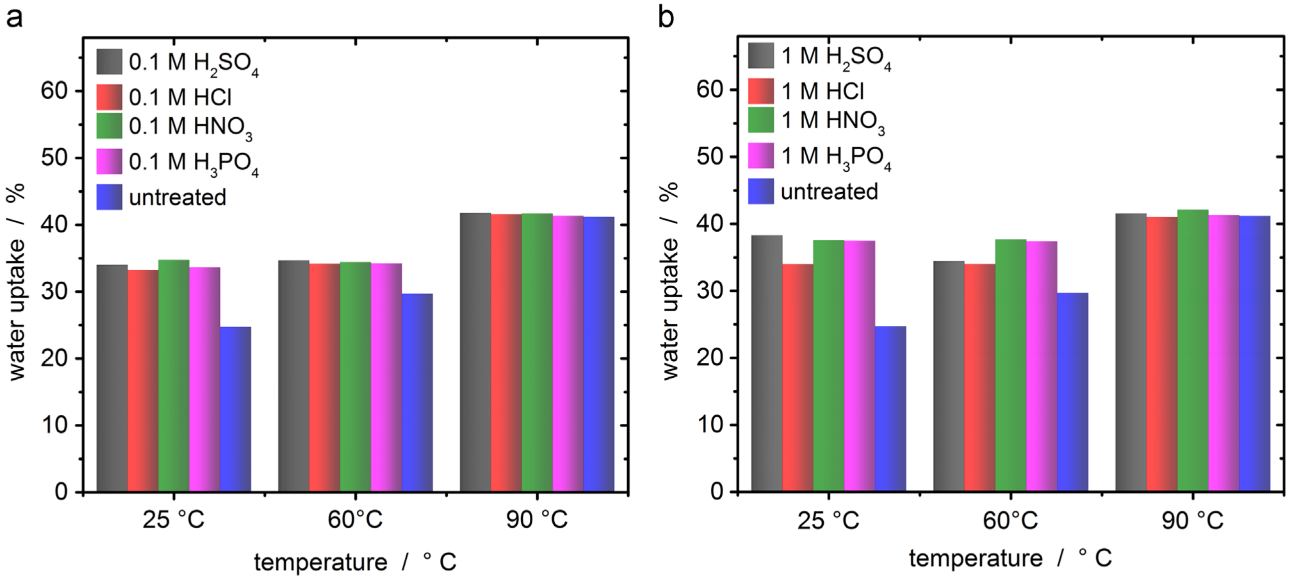

Fig. 5. Water uptake for membranes pretreated with different acids and acid concentrations (a) with 0.1 M acids, (b) with 1.0 M acids.

trends as for the WU at 0.1 M are observable, although the absolute values are slightly higher.

Since the membranes were all pretreated at a temperature of 80 °C, the influence of the pretreatment is no longer visible at higher measurement temperature (90 °C). Here, the WU increases significantly (41.5%) independent of the chosen acid or concentration. Therefore, we assume that the WU is merely a thermal effect above the pretreatment temperature. This is confirmed by the increasing WU of the untreated membrane, which was not exposed to thermal treatment before the WU measurements. It is well known from literature, that thermal treatment of the ionic clusters and channels in the Nafion® membrane results in an increase of volume available for WU [17,26,48,52]. Thus, all membranes pretreated at 80 °C maintain the expansion of channels and clusters although they were stored at room temperature before WU measurements, i.e. they exhibit the well known memory effect [39]. The thermal history of the Nafion® membranes could be erased by hydration at high temperature and high pressure in an autoclave as described by di Noto et al. [13,53,54]. This procedure leads to membranes with reproducible properties, which are determined by temperature and humidity during the autoclaving step. Since the present paper focuses on the different acidic pretreatments, this additional step was not implemented in order to make differences of the membrane properties visible.

3.1.3. Water vapor adsorption

In addition to liquid water uptake, adsorption of water vapor is important during fuel cell operation since the educt gases are usually humidified. Therefore, adsorption isotherms with vapor water as adsorbant give quantitative information about the amount of adsorbed water at varying relative pressures. This can be regarded as equivalent to the relative humidity in the membrane. Furthermore, the λ value $[\mathrm{mmol}_{H_2O} g^{-1}_{SO_3H}]$ can be estimated by taking into account the adsorbed water vapor amount, the IEC and the density of water at 10 °C as described by Eq. (4) [45]:

$$\lambda = \frac{m_{ads} \cdot \rho_{H_2O}}{M_{H_2O} \cdot \mathrm{IEC}_{acid}} \tag{4}$$

The adsorption isotherms for the membranes pretreated with 1 M H_2SO_4 and 1 M HCl are depicted in Fig. 6 in comparison to the untreated membrane. It can be seen that the membrane pretreated with 1 M H_2SO_4 exhibits the highest λ of 14.4 at a relative pressure of 1 (HCl: λ=13, untreated: λ=12.3). This is in good agreement with data reported by Weber et al. [48]. The smallest value and hence the smallest water vapor uptake per SO_3 -molecule in Nafion® is observed for the untreated membrane. These results are in good accordance with the WU measurements (cf. Fig. 5b), where a WU of 38.3% for 1 M H_2SO_4, 34% for 1 M HCl, and 24.7% for the untreated membrane were determined at 25 °C.

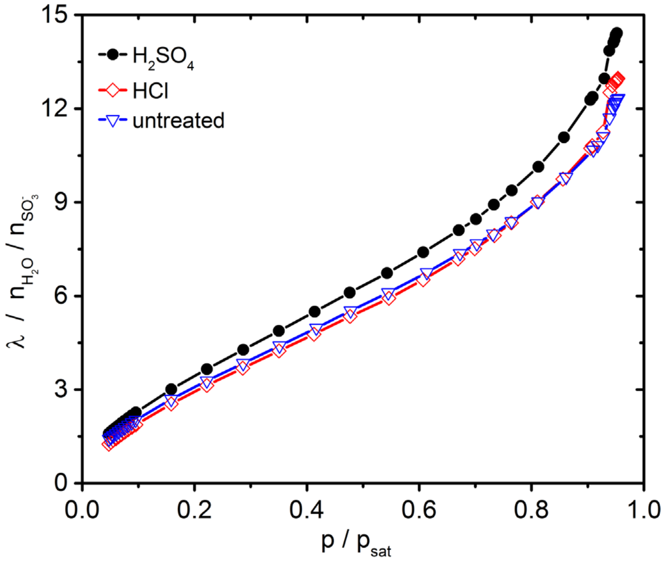

Fig. 6. Calculated λ values from water–vapor sorption isotherms conducted at 10 °C for membranes pretreated with different 1 M acids.

3.1.4. Differential-scanning calorimetry

The DSC curves depicted in Fig. 7a reveal an endothermic peak between 50 and 160 °C which can be attributed to the removal and evaporation of adsorbed water [55]. This peak is no longer visible in the second heating curve (not shown here). By integration of the peak area one obtains the evaporation enthalphy which indicates the state of hydration of the membrane [56]. Another explanation for the endothermic peak in this temperature range was given by Di Noto et al. and Page et al. who assigned the peak to a melting of small and imperfect fluorocarbon nanocrytalline domains of Nafion [13,54,57]. These nanocrystalline domains arise

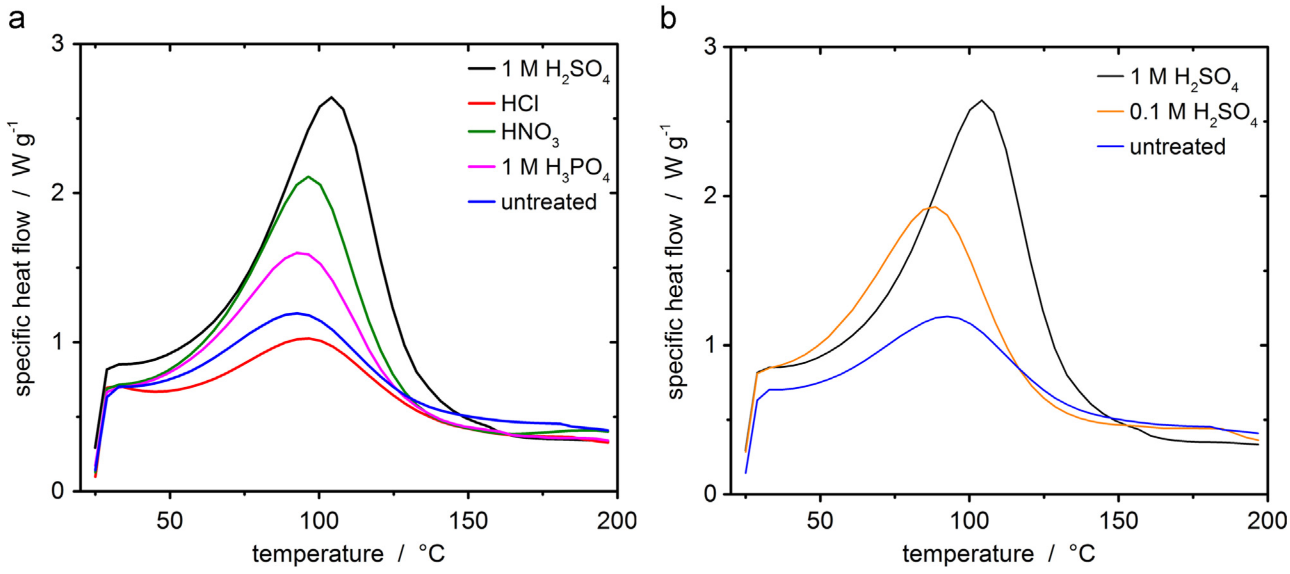

Fig. 7. DSC measurement spectra for membranes pretreated with different acids, (a) for different 1 M acids, (b) for different sulfuric acid concentrations.

due to the presence of the hydrogen-bonding interactions between the acid groups in the polar domains, which reduce the size of the ordered microdomains of the polymer matrix [13,58,59].

The resulting values are summarized in Table 4. For pretreatment with 1 M H_2SO_4 the highest value is observed while 1 M HCl results in an enthalpy that is by a factor of 4 smaller. Obviously, the evaporation enthalphy from DSC measurements match well with the liquid water uptake results. The influence of the acid concentration which is depicted exemplarily for membranes pretreated with H_2SO_4 in Fig. 7b is also in good agreement with the liquid water uptake measurements, where the membrane pretreated with 1 M H_2SO_4 exhibited a higher WU than the membrane pretreated with 0.1 M H_2SO_4. Di Noto et al. [13] reported a very similar peak temperature of 104 °C for a 1 M H_2SO_4 pretreated Nafion® membrane, although different heating rates have been used (di Noto et al.: 3 K min^{-1}, this paper: 10 K min^{-1}).

Table 4
Maximal temperature at the endothermic peaks during DSC measurements and calculated evaporation enthalphy.

Pretreatment	Evaporation enthalphy/J g^{-1}	Temperature/°C
1 M H_2SO_4	528.7	103.8
1 M HNO_3	413.4	96.8
0.1 M H_2SO_4	347.7	87.3
1 M H_3PO_4	322.3	93.6
Untreated	182.6	92.8
1 M HCl	137.7	96.0

3.1.5. FT-infrared spectroscopy of pretreated Nafion® membranes

The FT-IR spectra depicted in Fig. 8 reveal structural information about Nafion® pretreated with different acids and acid concentrations. Acording to Negro et al. [60] the FT-IR-spectra vary significantly dependent on the hydration state of the Nafion® membrane. In these measurements, dry Nafion® membranes did not exhibit a peak at wavelengths higher 3000 cm^{-1} and at ca. 1700 cm^{-1}. In this contribution, the FT-IR spectra of all membranes were taken in a wet ($\lambda=22$) condition which can be confirmed since peaks at ca. 1700 cm^{-1} and higher 3000 cm^{-1} (not shown here) are visible. The measured spectra are in good agreement with the work of Laporta et al. [61]. The FT-IR spectra will be described in the following starting at small wavelengths. As already shown by Laporta et al. [61] no absorption band is visible in the range of 920–930 cm^{-1} which would correspond to the S-O stretching band of the protonated SO_3H group. This band is only visible if the membrane is entirely dehydrated in the absence of even trace amounts of water. The absorption band at ca. 982 cm^{-1} corresponds to the C–F stretching band of the perfluorinated backbone in Nafion®. The absorption band at 1057 cm^{-1} is associated with the symmetric S-O stretching band while at 1304 cm^{-1} the asymmetric strechting band of the deprotonated SO_3^- group appears. Furthermore two broad absorption bands at 1229 cm^{-1} and 1156 cm^{-1} are visible which correspond to symmetric and asymmetric C-F stretching, respectively. Due to their width, parts of the SO_3 band are overlapped. The membrane pretreated with HNO_3 exhibits the lowest intensity in the absorption range of 1229–1156 cm^{-1} while the H_2SO_4 treated membrane, for both concentrations, has the highest intensity, followed by HCl, H_3PO_4 and the untreated membrane, respectively. The absorption band at 1420 cm^{-1} in Fig. 8 is caused by the combination of C-F-groups in amorphous polytetrafluorethylene. Here, no significant influence of the pretreatment is detectable. At 1740 cm^{-1} the shear vibration of the water molecules in the so-called Zundel-ion $H_5O_2^+$ [61] is visible. The intensities vary with the pretreatment procedure. Hydronium ions H_3O^+ cannot be detected in this absorption range which would be expected at low humidification of the membrane (at 1710 cm^{-1}). As reported by Leuchs et al. [62] the formation of Zundel ions only occurs if $\lambda \geq 2$. In the presence of water excess the intensity of the Zundel ion band decreases due to a dilution effect. It can therefore be concluded that the λ-value is higher than 2 and that the formation of Zundel ions is possible. The IR spectra show an influence of the pretreatment procedure to the intensity of the deprotonated SO_3^-

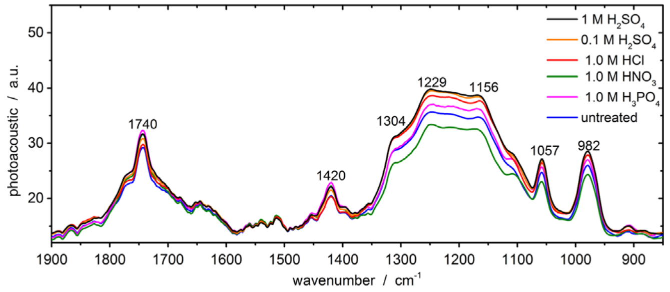

Fig. 8. FT-IR spectra for Nafion® pretreated with different acids.

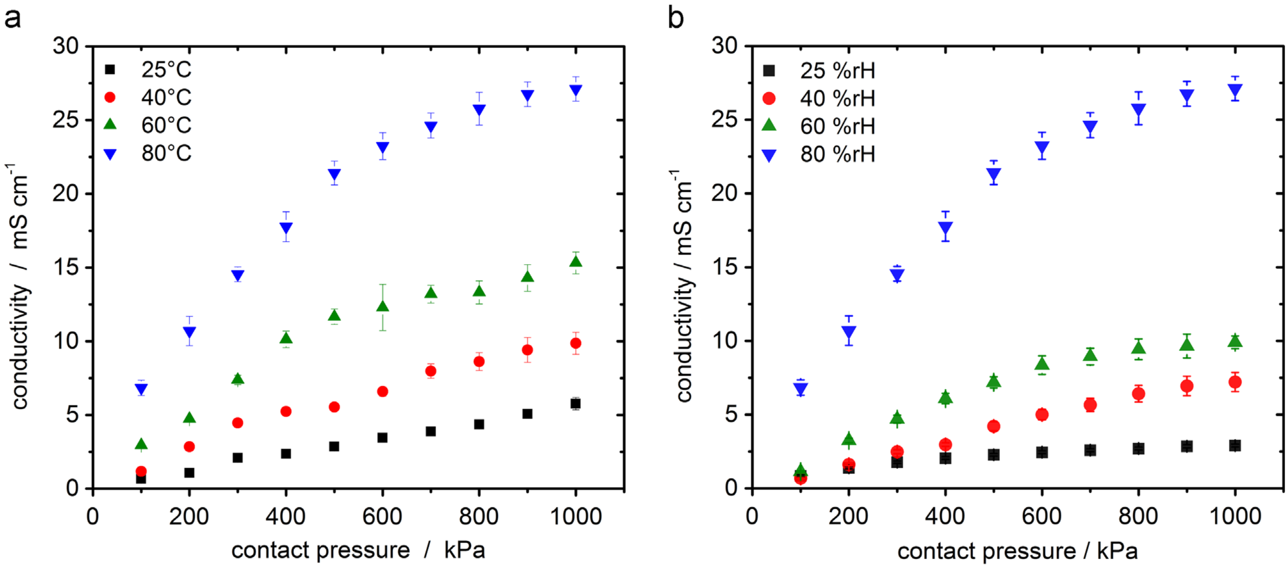

Fig. 9. Conductivity of 1 M H_2SO_4 pretreated membranes, (a) at 80%rH and different temperatures (25, 40, 60, 80 °C), (b) at 80 °C and different humidities (25, 40, 60, 80%rH).

groups. In contrast, no influence to the intensities of the backbone from the Nafion® membrane was observed.

3.2. Ionic conductivity

In Fig. 9 the results of the conductivity measurements for the membrane pretreated with 1 M H_2SO_4 are depicted. Fig. 9a shows the ionic conductivity vs. the contact pressure at different temperatures for 80%rH. The maximal conductivity (27.1 S cm^{-1}) is achieved at a temperature of 80 °C and a contact pressure of 1000 kPa. Furthermore, the conductivity at 1000 kPa and 80 °C is five times higher than at 25 °C. It is obvious that a high contact pressure is beneficial for a high conductivity. Moreover, a contact pressure of 1000 kPa corresponds to a typical assembly pressure in fuel cells and electrolyzers [63]. The activation energy can be estimated from the temperature dependency of the ionic conductivity by applying an Arrhenius approach [17,24,64]. This activation energy corresponds to the proton transport through Nafion®. At all considered relative humidities (Fig. 9b) and temperatures, the activation energy is on average 20.73 ± 1.98 kJ mol^{-1}, which is in good agreement with literature data reported by Slade et al. [55]. Giffin et al. [14] estimated similar activation energies in the range of 10–25 kJ mol^{-1}. However, these data cannot be directly compared since the VTF approach was used. The influence of water content on the activation energy is considered as secondary effect in this temperature range (25–80 °C) and can be hence neglected [65,66].

The activation energy for the proton-hopping Grotthuss mechanism is ca. 11 kJ mol^{-1} and thus below the activation energy determined in our investigation [11,12]. The higher activation energy can be attributed to the fact that the major part of the proton conductivity is due to the vehicle mechanism rather than to the proton-hopping mechanism at the considered temperatures [12]. This interpretation is in good accordance with the structural information obtained from the FT-IR spectra (Fig. 8).

In Fig. 9b the conductivity as a function of relative humidity and contact pressure at a constant temperature of 80 °C is depicted. The conductivity increases with rising relative humidity. For example, the conductivity at 80%rH and a contact pressure of 1000 kPa (27.1 mS cm^{-1}) is nearly ten times higher than at 25%rH (2.9 mS cm^{-1}). The rather low conductivity at 25%rH can be attributed to the phenomenon described by Morris et al. [21]. These authors stated that the swelling of Nafion® commences at a λ value of 1.9, being a threshold for the insulator-to-conductor transition. As soon as this value is achieved, proton conductivity is ensured since the sulfonic acid groups are hydrated and accordingly the channels in Nafion® are formed [21]. Through application of the mathematical model of Weber et al. [48] (cf. Appendix) a λ value at 80 °C and 25%rH of approximately 2.1 is obtained. Hence, the membrane starts to swell at these conditions and subsequently channels for proton transport are barely formed explaining the low initial conductivity.

In Fig. 10 the conductivity measurements for the membranes pretreated with HNO_3 (0.1 M and 1 M) at 40%rH and 80%rH at a constant temperature of 60 °C are summarized. For comparison the conductivity of the untreated membrane is also included. The conductivities are very similar up to contact pressures of 400 kPa as can be seen from Fig. 10a. Only at even higher contact pressure the membrane pretreated with 1 M HNO_3 (5.48 mS cm^{-1}) reaches a 25% higher conductivity than the membrane pretreated with 0.1 M HNO_3 (4.38 mS cm^{-1}) and a 31.5% higher conductivity than the untreated membrane (4.17 mS cm^{-1}) at 1000 kPa. Upon increasing the humidity from 40%rH to 80%rH (Fig. 10b) the conductivity of the membrane pretreated with 1 M HNO_3 increases drastically by 160% to 14.2 mS cm^{-1}. Moreover, the deviation between the membranes pretreated with 0.1 M HNO_3 and 1 M HNO_3 is substantially lower (12.7%) at 80%rH. In addition, the untreated membrane exhibits a similar conductivity as the membrane pretreated with 1 M HNO_3 at 1000 kPa. In conclusion the pretreatment of Nafion® membranes with 1 M HNO_3 only has a positive effect on the conductivity at low relative humidity (40%rH).

In Fig. 11 the results of conductivity measurements for the membranes pretreated with H_3PO_4 are depicted. At low relative humidities (Fig. 11a, 40%rH) a similar trend as for the membrane pretreated with HNO_3 is found. Here, the conductivity of the membrane pretreated with 1 M H_3PO_4 (5.9 mS cm^{-1}) is by 57% higher than after treatment with 0.1 M H_3PO_4 (3.8 mS cm^{-1}) at 1000 kPa. Furthermore, the membrane pretreated with 1 M H_3PO_4 exhibits a 42°% higher conductivity than the untreated membrane. Upon increasing the relative humidity to 80%rH (Fig. 11b) an increase of the conductivity of the membrane pretreated with 1 M H_3PO_4 by 140% to 14.3 S cm^{-1} is measured at 1000 kPa. In contrast the influence of the concentration at higher relative humidities is negligible since the conductivities of the untreated membrane and the membrane preatreated with H_3PO_4 are comparable. Hence, also the pretreatment with H_3PO_4 only yields a positive effect at

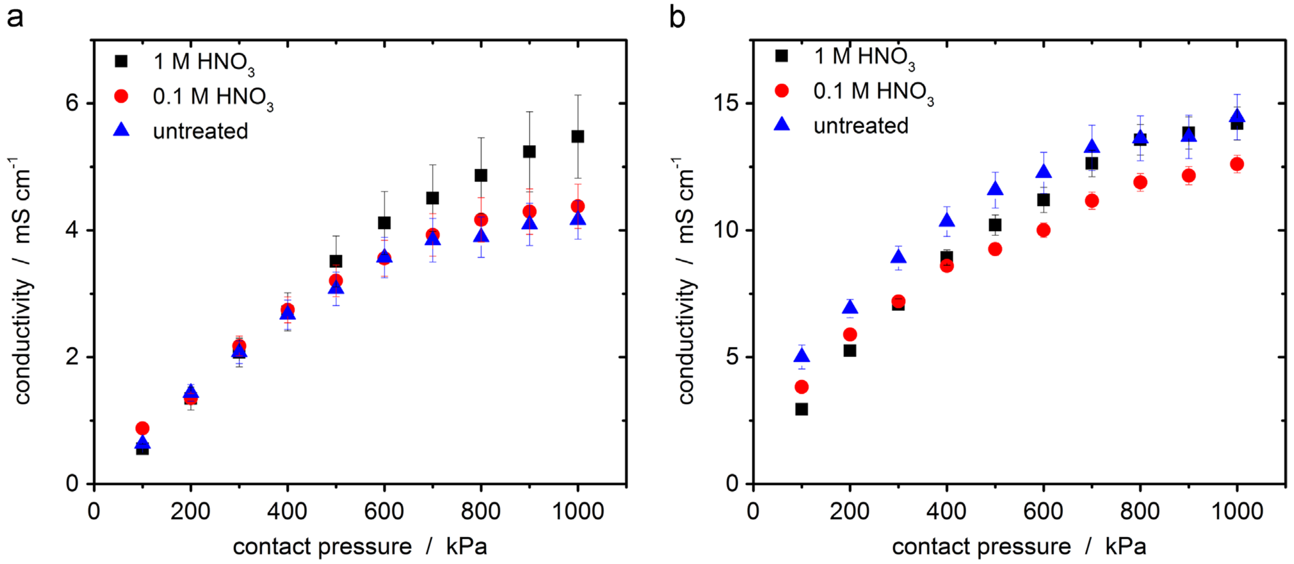

Fig. 10. Conductivity for HNO_3 (0.1 M and 1 M) pretreated membranes at 60 °C, (a) at 40%rH, (b) at 80%rH.

low relative humidities.

In Fig. 12 the results of the conductivity measurements for different acids and acid concentrations at 60 °C, 1000 kPa and different relative humidites (40, 80, 100%rH) are compared. The conductivity of all membranes increases nonlinearly with rising relative humidity which can be explained by the percolation theory [67].

The conductivities σ at a relative humidity of 40%rH are in most cases higher than the conductivity of the untreated membrane. Only for the membrane pretreated with 0.1 M HCl was a comparable value observed. The achievable increase in conductivity after pretreatment is 21.4% (1 M H_2SO_4) and 23.8% (1 M HCl). The conductivity at 40%rH and 1000 kPa increases in the following order:

σ(0.1 M HCl < untreated < 1 M H_2SO_4 < 0.1 M H_2SO_4 = 1 M HNO_3 < 1 M H_3PO_4 < 1 M HCl)

At a higher relative humidity of 80%rH, the positive effect of the pretreatment is significantly diminished. At these conditions, only the membrane pretreated with 1 M H_2SO_4 exhibits a conductivity that is 6% higher than for the untreated membrane. The membranes pretreated with the other acids (1 M HNO_3 and 1 M H_3PO_4) either show the same conductivity or even lower values than the untreated membrane.

Thus, the conductivity at 80%rH and 1000 kPa increases in the following order:

σ(0.1 M HCl < 1 M HCl < 0.1 M H_2SO_4 < 1 M HNO_3 = 1 M H_3PO_4 = untreated < 1 M H_2SO_4)

Significant changes occur if the relative humidity is further increased form 80%rH to 100%rH. Here, all membranes exhibit higher conductivities than the untreated membrane except for the membrane pretreated with 1 M HNO_3 (-20.6%). While the membranes pretreated with 1 M H_2SO_4 and 1 M H_3PO_4 only show a slight conductivity increase (4.3% and 5.7%, respectively), larger improvements were achieved for membranes pretreated with 0.1 M H_2SO_4 (24.7%), 1 M HCl (22.8%) and 0.1 M HCl (34.2%). This enhancement is remarkable since for these membranes the lowest conductivity among all pretreated membranes was observed at lower relative humidities. These results are in good accordance with the ionic exchange capacities (cf. Fig. 4). Obviously, the ionic conductivity strongly depends on the amount of protonated sulfonic groups in Nafion®. Therefore, the pK_a value of the applied acid during pretreatment is a key parameter for a high ionic

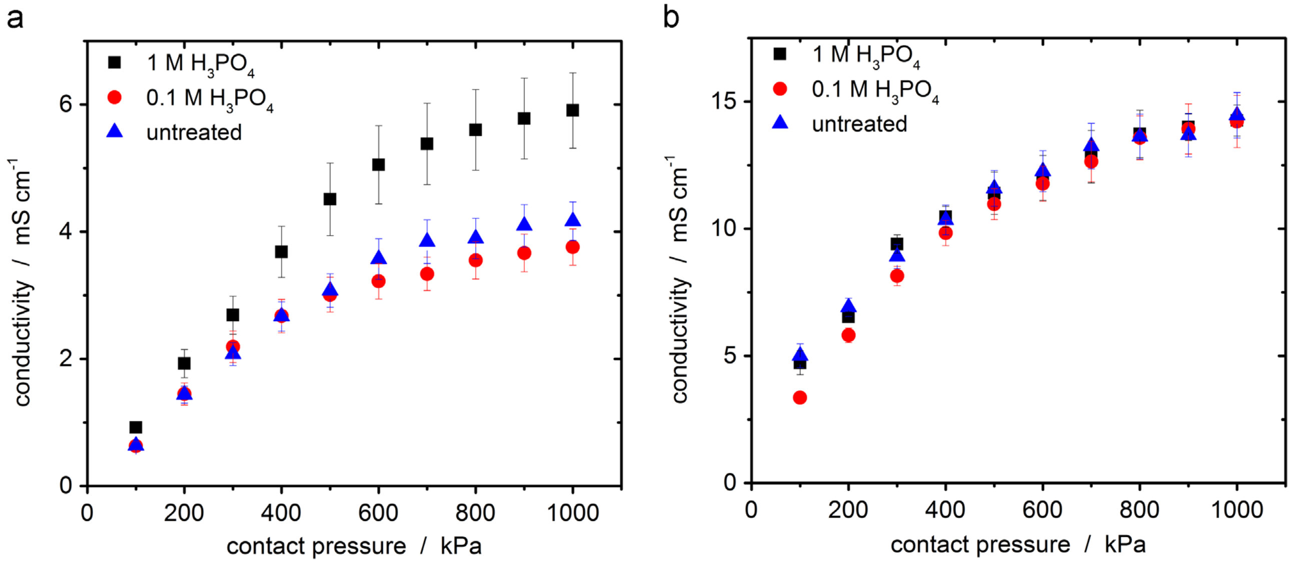

Fig. 11. Conductivity for H_3PO_4 (0.1 M and 1 M) pretreated membranes at 60 °C, (a)at 40 %rH, (b) at 80%rH

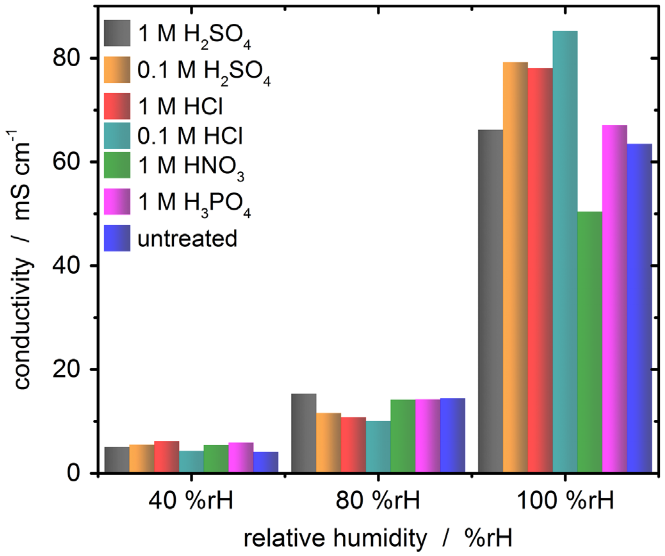

Fig. 12. Conductivity measurements for different pretreated membranes at 60 °C, 1000 kPa.

conductivity in the resulting pretreated membrane. Furthermore, treatment with diluted acids (0.1 M) results only at 100%rH in an improvement of conductivity. Hence, pretreatment with 0.1 M H_2SO_4 or with HCl (either 0.1 M or 1 M) is recommended in order to achieve an optimal conductivity of membranes at high relative humidities and temperatures employed for fuel cells or electrolyzers.

4. Conclusion

In the present contribution the influence of acid pretreatment of Nafion® membranes on the resulting IEC, WU and ionic conductivity was systematically investigated. For this purpose, an appropriate experimental setup was developed which allows the measurement of the ionic conductivity under varying conditions (relative humidity, temperature and contact pressure) with the aid of electrochemical impedance spectroscopy. The pK_a value and the concentration of the used acid were identified as the major factors influencing the ion exchange capacity. In addition, the temperature during the pretreatment procedure is decisive for the water uptake. Here, the influence of the acid type or the acid concentration is of secondary importance. Overall, the combination of high temperature, relative humidity and contact pressure is beneficial for a resulting high ionic conductivity of Nafion® membranes.

Acknowledgments

The authors authors gratefully acknowledge the German Research Foundation (Deutsche Forschungsgemeinschaft, DFG) for financial support of this research work under the project KU 853/5-1.

Appendix.A

Table A.1

Table A.1
Adjusted parameters for the chemical model of water uptake from the vapor phase, taken from Meyers and Newman [68].

Parameter	Value
K_1	100
K_2	0.217
$E^*_{0,0}$	$-$ 41.7 g mol^{-1}
E^*_{0,H_3O^+}	$-$ 52.0 g mol^{-1}
$E^*_{H_3O^+,H^+}$	$-$ 3721.6 g mol^{-1}

For determination of the membrane thickness as a function of the relative humidity and temperature a mathematical model reported by Weber et al. was used [48]. These authors suggest a chemical model to describe the water transport in a vapor-equilibrated Nafion® membrane. Therefore, the hydration of sulfonic acid sites in the membrane clusters (λ) was used to calculate water uptake isotherms as a function of vapor activity. A modification of the chemical model described by Meyers and Newman [68] was used to express the electrochemical potentials for multi-component transport in polymer electrolyte membranes (Eq. (A.1) and Eq. (A.2)). Both equations need to be solved simultaneously.

$$K_1 = \frac{\lambda_{H_3O^+}}{(1-\lambda_{H_3O^+})\bullet(\lambda - \lambda_{H_3O^+})}\bullet\exp(\phi_1\bullet\lambda_{H_3O^+})\bullet\exp(\phi_2\bullet\lambda) \tag{A.1}$$

$$a_0 = K_2\bullet(\lambda - \lambda_{H_3O^+})\bullet\exp(\phi_2\bullet\lambda_{H_3O^+})\bullet\exp(\phi_3\bullet\lambda) \tag{A.2}$$

The molar ratio of hydronium ions and sulfonic acid sites is expressed by $\lambda_{H_3O^+}$, EW is the equivalent weight of the membrane (1100 g equiv^{-1} for Nafion® 117), λ_i^* describes the secondary reference-state quantity for species i and $E^*_{i,j}$ is an interaction parameter between species i and j (Eqs. (A.3)–(A.7)).

$$K_1 = \frac{\lambda^*_{H_3O^+}}{\lambda_0^*\bullet\lambda^*_{H^+}} \tag{A.3}$$

$$K_2 = \frac{\lambda^*_{H^+}}{EW}\bullet\exp\left(-\frac{\mu_0^{ref}}{RT}\right) \tag{A.4}$$

$$\phi_1 = \frac{2}{EW}\bullet(E^*_{0,0}-2E^*_{H_3O^+,H^+}-2E^*_{0,H_3O^+}) \tag{A.5}$$

$$\phi_2 = \frac{2}{EW}\bullet(E^*_{0,H_3O^+} - E^*_{0,0}) \tag{A.6}$$

$$\phi_2 = \frac{2E_{0,0}}{EW} \tag{A.7}$$

The parameters given in Table A.1 were used by Weber et al. [48] to fit the experimental data from Zawodzinski et al. [17]. The temperature dependence was simplified assuming that all parameters are independent of the temperature except K_2. Therefore, an Arrhenius approach was applied (Eq. (A.8)).

$$K_2 = 0.217\bullet\exp\left[\frac{1000}{R}\bullet\left(\frac{1}{T_{ref}} - \frac{1}{T}\right)\right] \tag{A.8}$$

An empirical correction of $\lambda$is used (Eq. (A.9)) to take into account the influence of the higher binding energy at low λ_0 values.

$$\lambda = \lambda_0\bullet[1 + \exp(0.3-\lambda_0)] \tag{A.9}$$

With the above equations the water content of a Nafion® membrane can be calculated taking into account water activity and temperature. The λ value varies from 0 to 14 for a vapor-equilibrated membrane with decreasing λ values at rising temperatures. For determination of the membrane thickness as a function of λ it is assumed that the membrane is able to swell unrestrained. The volume (V) of a swelling membrane (Eq. (A.10)) can be obtained with the partial molar volume of the dry membrane (V_m), λ and the partial molar volume of water ($\bar{V}_0$).

$$V = \bar{V}_m + \lambda \cdot \bar{V}_0 \tag{A.10}$$

The partial molar volume of the dry membrane (Eq. (A.11)) can be calculated by the equivalent weight (EW) of the used Nafion® membrane (1100 g equiv^{-1}) and $\rho_{m,o}$ as the dry density of the membrane (2 g cm^{-3}) [21].

$$\bar{V}_m = \frac{EW}{\rho_{m,o}} \tag{A.11}$$

The partial molar volume of water (V_0) is the ratio of molar mass of water (M_0) and temperature dependent density of water (ρ_0) as described by Eq. (A.12).

$$\bar{V}_0 = \frac{M_0}{\rho_0} \tag{A.12}$$

Since the molar volumes and the λ value are known, the change of the thickness with water content of the swelling membrane can be calculated (Eq. (A.13)). The prefactor of 0.36 in Eq. (A.13) results from the anisotropic nature of Nafion®; in contrast an isotropic membrane would swell with a factor of 0.29. The thickness of the dry membrane (l_0) is 177.8 μm for Nafion® 117 and $\hat{\lambda}$ is the average value of λ in the membrane which is assumed to be constant for a vapor-equilibrated membrane at a certain water vapor activity and temperature.

$$l = l_0 \cdot \left(1 + 0.36 \cdot \frac{\hat{\lambda} \cdot \bar{V}_0}{\bar{V}_m}\right) \tag{A.13}$$

The thickness decreases with increasing temperature and increases with increasing water vapor activity (a_{water}). As a result, the calculated thickness increases from 182.23 μm for $a_{water} = 0.25$ at 80 °C to 206.45 μm for $a_{water} = 1$ at 25 °C.

References

[1] T. Vidakovic-Koch, I. Gonzalez Martinez, R. Kuwertz, U. Kunz, T. Turek, K. Sundmacher, Electrochemical membrane reactors for sustainable chlorine recycling, Membranes 2 (2012) 510–528.

[2] M.L. Perry, T.F. Fuller, A. Historical, Perspective of fuel cell technology in the 20th Century, J. Electrochem. Soc. 149 (2002) S59–S67.

[3] R. Kuwertz, I.G. Martinez, T. Vidakovic-Koch, K. Sundmacher, T. Turek, U. Kunz, Energy-efficient chlorine production by gas-phase HCl electrolysis with oxygen depolarized cathode, Electrochem. Commun. 34 (2013) 320–322.

[4] W. Grot, Perfluorinated ion-exchange membranes of high chemical and thermal-stability, Chem. Ingenieur Tech. 44 (1972) 167–169.

[5] W.G.T. Bisot, P.Resnick, E.I. Du Pont de Nemours and Company, Membrane, electrochemical cell and electrolysis process, US4437951, 20.03.1984.

[6] W.Grot, CF2=CFCF2CF2SO2F and Related Fluorocarbon Vinyl Compounds, CA883324, 12.10.1971.

[7] W.Grot, Electrochemical Cell Containing a Water-Wettable Polytetrafluoroethylene Separator, US3702267, 07.11.1972.

[8] J.T. Hinatsu, M. Mizuhata, H. Takenaka, Water uptake of perfluorosulfonic acid membranes from liquid water and water vapor, J. Electrochem. Soc. 141 (1994) 1493–1498.

[9] T.D. Gierke, G.E. Munn, F.C. Wilson, The morphology in nafion perfluorinated membrane products, as determined by wide- and small-angle x-ray studies, J. Polym. Sci.: Polym. Phys. Ed. 19 (1981) 1687–1704.

[10] W.Y. Hsu, T.D. Gierke, Ion-transport and clustering in nafion perfluorinated membranes, J. Membr. Sci. 13 (1983) 307–326.

[11] N. Agmon, The Grotthuss mechanism, Chem. Phys. Lett. 244 (1995) 456–462.

[12] A.A. Kornyshev, A.M. Kuznetsov, E. Spohr, J. Ulstrup, Kinetics of proton transport in water, J. Phys. Chem. B 107 (2003) 3351–3366.

[13] V. Di Noto, M. Piga, G.A. Giffin, K. Vezzù, T.A. Zawodzinski, Interplay between mechanical, electrical, and thermal relaxations in nanocomposite proton conducting membranes based on nafion and a $[(ZrO_2)\cdot(Ta_2O_5)0.119]$ core–shell nanofiller, J. Am. Chem. Soc. 134 (2012) 19099–19107.

[14] G.A. Giffin, G.M. Haugen, S.J. Hamrock, V. Di Noto, Interplay between structure and relaxations in perfluorosulfonic acid proton conducting membranes, J. Am. Chem. Soc. 135 (2013) 822–834.

[15] P. Schroeder, Über Erstarrungs- und Quellungserscheinungen von Gelatine, Z. Phys. Chem. 45 (1903) 57.

[16] C. Vallieres, D. Winkelmann, D. Roizard, E. Favre, P. Scharfer, M. Kind, On Schroeder's paradox, J. Membr. Sci. 278 (2006) 357–364.

[17] T.A. Zawodzinski, C. Derouin, S. Radzinski, R.J. Sherman, V.T. Smith, T. E. Springer, S. Gottesfeld, Water-uptake by and transport through Nafion® 117 membranes, J. Electrochem. Soc. 140 (1993) 1041–1047.

[18] M.W. Verbrugge, E.W. Schneider, R.S. Conell, R.F. Hill, The effect of temperature on the equilibrium and transport-properties of saturated poly(Perfluorosulfonic Acid) membranes, J. Electrochem. Soc. 139 (1992) 3421–3428.

[19] H. Takata, N. Mizuno, M. Nishikawa, S. Fukada, M. Yoshitake, Adsorption properties of water vapor on sulfonated perfluoropolymer membranes, Int. J. Hydrogen Energy 32 (2007) 371–379.

[20] T. Okada, G. Xie, O. Gorseth, S. Kjelstrup, N. Nakamura, T. Arimura, Ion and water transport characteristics of Nafion membranes as electrolytes, Electrochim. Acta 43 (1998) 3741–3747.

[21] D.R. Morris, X. Sun, Water-sorption and transport properties of Nafion 117, J. Appl. Polym. Sci. 50 (1993) 1445–1452.

[22] T.A. Zawodzinski, M. Neeman, L.O. Sillerud, S. Gottesfeld, Determination of water diffusion-coefficients in perfluorosulfonate ionomeric membranes, J. Phys. Chem. 95 (1991) 6040–6044.

[23] A.V. Anantaraman, C.L. Gardner, Studies on ion-exchange membranes.1. Effect of humidity on the conductivity of Nafion®, J. Electroanal. Chem. 414 (1996) 115–120.

[24] M. Cappadonia, J.W. Erning, S.M.S. Niaki, U. Stimming, Conductance of Nafion-117 membranes as a function of temperature and water-content, Solid State Ion. 77 (1995) 65–69.

[25] V. Di Noto, N. Boaretto, E. Negro, G. Pace, New inorganic–organic proton conducting membranes based on Nafion and hydrophobic fluoroalkylated silica nanoparticles, J. Power Sources 195 (2010) 7734–7742.

[26] T.A. Zawodzinski, T.E. Springer, J. Davey, R. Jestel, C. Lopez, J. Valerio, S. Gottesfeld, A comparative-study of water-uptake by and transport through ionomeric fuel-cell membranes, J. Electrochem. Soc. 140 (1993) 1981–1985.

[27] E.A. Ticianelli, C.R. Derouin, S. Srinivasan, Localization of platinum in low catalyst loading electrodes to to attain high power densities in SPE fuel cells, J. Electroanal. Chem. Interfacial Electrochem. 251 (1988) 275–295.

[28] M.B. Satterfield, J.B. Benziger, Viscoelastic properties of Nafion at elevated temperature and humidity, J. Polym. Sci. Pol. Phys. 47 (2009) 11–24.

[29] K. Hongsirikarn, J.G. Goodwin, S. Greenway, S. Creager, Influence of ammonia on the conductivity of Nafion membranes, J. Power Sources 195 (2010) 30–38.

[30] P.D. Beattie, V.I. Basura, S. Holdcroft, Temperature and pressure dependence of O_2 reduction at Pt | Nafion® 117 and Pt | BAM® 407 interfaces, J. Electroanal. Chem. 468 (1999) 180–192.

[31] V.I. Basura, P.D. Beattie, S. Holdcroft, Solid-state electrochemical oxygen reduction at Pt | Nafion® 117 and Pt |BAM3G™ 407 interfaces, J. Electroanal. Chem. 458 (1998) 1–5.

[32] K. Broka, P. Ekdunge, Oxygen and hydrogen permeation properties and water uptake of Nafion® 117 membrane and recast film for PEM fuel cell, J. Appl. Electrochem. 27 (1997) 117–123.

[33] M.B. Satterfield, P.W. Majsztrik, H. Ota, J.B. Benziger, A.B. Bocarsly, Mechanical properties of Nafion and titania/Nafion composite membranes for polymer electrolyte membrane fuel cells, J. Polym. Sci. Pol. Phys. 44 (2006) 2327–2345.

[34] G.S. Hwang, M. Kaviany, J.T. Gostick, B. Kientiz, A.Z. Weber, M.H. Kim, Role of water states on water uptake and proton transport in Nafion using molecular simulations and bimodal network, Polymer 52 (2011) 2584–2593.

[35] Q.M. Huang, Q.L. Zhang, H.L. Huang, W.S. Li, Y.J. Huang, J.L. Luo, Methanol permeability and proton conductivity of Nafion membranes modified electrochemically with polyaniline, J. Power Sources 184 (2008) 338–343.

[36] P.W. Majsztrik, M.B. Satterfield, A.B. Bocarsly, J.B. Benziger, Water sorption, desorption and transport in Nafion membranes, J. Membr. Sci. 301 (2007) 93–106.

[37] T. Kinumoto, M. Inaba, Y. Nakayama, K. Ogata, R. Umebayashi, A. Tasaka, Y. Iriyama, T. Abe, Z. Ogumi, Durability of perfluorinated ionomer membrane against hydrogen peroxide, J. Power Sources 158 (2006) 1222–1228.

[38] M. Bass, V. Freger, Hydration of Nafion and Dowex in liquid and vapor environment: Schroeder's paradox and microstructure, Polymer 49 (2008) 497–506.

[39] G. Gebel, Structural evolution of water swollen perfluorosulfonated ionomers from dry membrane to solution, Polymer 41 (2000) 5829–5838.

[40] F. Bauer, S. Denneler, M. Willert-Porada, Influence of temperature and humidity on the mechanical properties of Nafion® 117 polymer electrolyte membrane, J. Polym. Sci. Part B: Polym. Phys. 43 (2005) 786–795.

[41] M. Hara, J. Inukai, K. Miyatake, H. Uchida, M. Watanabe, Temperature dependence of the water distribution inside a Nafion membrane in an operating polymer electrolyte fuel cell. A micro-Raman study, Electrochim. Acta 58 (2011) 449–455.

[42] J. Ramkumar, T. Mukherjee, Effect of aging on the water sorption and ion exchange studies on Nafion and Dowex resins: transition metal ions-proton exchange systems, Sep. Purif. Technol. 54 (2007) 61–70.

[43] T.Y. Soboleva, Z. Xie, Z.Q. Shi, E. Tsang, T.C. Navessin, S. Holdcroft, Investigation of the through-plane impedance technique for evaluation of anisotropy of proton conducting polymer membranes, J. Electroanal. Chem. 622 (2008) 145–152.

[44] R. Savinell, E. Yeager, D. Tryk, U. Landau, J. Wainright, D. Weng, K. Lux, M. Litt, C. Rogers, A polymer electrolyte for operation at temperatures up to 200 °C, J.

Electrochem. Soc. 141 (1994) L46–L48.
[45] S.J. Peighambardoust, S. Rowshanzamir, M. Amjadi, Review of the proton exchange membranes for fuel cell applications, Int. J. Hydrogen Energy 35 (2010) 9349–9384.
[46] V. Di Noto, J.J. Fontanella, M.C. Wintersgill, G.A. Giffin, K. Vezzù, M. Piga, E. Negro, Pressure, Temperature, and Dew Point Broadband Electrical Spectroscopy (PTD-BES) for the Investigation of Membranes for PEMFCs▴, Fuel Cells 13 (2013) 48–57.
[47] V.F. Lvovich, Impedance Spectroscopy: Applications to Electrochemical and Dieletric Phenomena, John Wiley& Sons Inc., Hoboken, New Jersey, 2012.
[48] A.Z. Weber, J. Newman, Transport in polymer-electrolyte membranes: II. Mathematical model, J. Electrochem. Soc. 151 (2004) A311–A325.
[49] A.Z. Weber, J. Newman, Transport in polymer-electrolyte membranes: I. Physical model, J. Electrochem. Soc. 150 (2003) A1008–A1015.
[50] E. Riedel, Anorganische Chemie, Walter de Gruyter & Co. KG, Berlin, 2004.
[51] C. Ma, L. Zhang, S. Mukerjee, D. Ofer, B. Nair, An investigation of proton conduction in select PEM's and reaction layer interfaces-designed for elevated temperature operation, J. Membr. Sci. 219 (2003) 123–136.
[52] G. Alberti, R. Narducci, M. Sganappa, Effects of hydrothermal/thermal treatments on the water-uptake of Nafion membranes and relations with changes of conformation, counter-elastic force and tensile modulus of the matrix, J. Power Sources 178 (2008) 575–583.
[53] V. Di Noto, M. Piga, L. Piga, S. Polizzi, E. Negro, New inorganic–organic proton conducting membranes based on Nafion® and [(ZrO2)·(SiO2)0.67] nanoparticles: Synthesis vibrational studies and conductivity, J. Power Sources 178 (2008) 561–574.
[54] V. Di Noto, M. Piga, S. Lavina, E. Negro, K. Yoshida, R. Ito, T. Furukawa, Structure, properties and proton conductivity of nanocomposite membranes, Electrochim. Acta 55 (2010) 1431–1444.
[55] L. Sun, J.S. Thrasher, Studies of the thermal behavior of Nafion® membranes treated with aluminum(III), Polym. Degrad. Stabil. 89 (2005) 43–49.
[56] S.H. de Almeida, Y. Kawano, Thermal Behavior of Nafion Membranes, J. Thermal Anal. Calorim. 58 (1999) 569–577.
[57] K.A. Page, K.M. Cable, R.B. Moore, Molecular origins of the thermal transitions and dynamic mechanical relaxations in perfluorosulfonate ionomers, Macromolecules 38 (2005) 6472–6484.
[58] V. Di Noto, N. Boaretto, E. Negro, P.E. Stallworth, S. Lavina, G.A. Giffin, S. G. Greenbaum, Inorganic–organic membranes based on Nafion, $[(ZrO_2)\cdot(HfO_2)0.25]$ nanoparticles. Part II: Relaxations and conductivity mechanism, Int. J. Hydrogen Energy 37 (2012) 6215–6227.
[59] V. Di Noto, N. Boaretto, E. Negro, G.A. Giffin, S. Lavina, S. Polizzi, Inorganic–organic membranes based on Nafion, $[(ZrO_2)\cdot(HfO_2)0.25]$ and $[(SiO_2)\cdot(HfO_2)0.28]$. Part I: Synthesis, thermal stability and performance in a single PEMFC, Int. J. Hydrogen Energy 37 (2012) 6199–6214.
[60] E. Negro, M. Vittadello, K. Vezzù, S.J. Paddison, V. Di Noto, The influence of the cationic form and degree of hydration on the structure of Nafion™, Solid State Ion. 252 (2013) 84–92.
[61] M. Laporta, M. Pegoraro, L. Zanderighi, Perfluorosulfonated membrane (Nafion): FT-IR study of the state of water with increasing humidity, Phys. Chem. Chem Phys 1 (1999) 4619–4628.
[62] M. Leuchs, G. Zundel, Easily polarizable hydrogen bonds in aqueous solutions of acids. Perchloric acid and trifluoromethane sulphonic acid, J. Chem. Soc. Faraday Trans. 2: Mol. Chem. Phys. 74 (1978) 2256–2267.
[63] L. Zhang, Y. Liu, H. Song, S. Wang, Y. Zhou, S.J. Hu, Estimation of contact resistance in proton exchange membrane fuel cells, J. Power Sources 162 (2006) 1165–1171.
[64] R.C.T. Slade, J. Barker, J.H. Strange, Protonic conduction and ^{1}H self-diffusion in Nafion film studied by ac conductivity and pulsed field gradient NMR Techniques, Solid State Ion. 35 (1989) 11–15.
[65] J. Halim, F.N. Buchi, O. Haas, M. Stamm, G.G. Scherer, Characterization of perfluorosulfonic acid membranes by conductivity measurements and small-angle X-Ray-scattering, Electrochim. Acta 39 (1994) 1303–1307.
[66] M. Cappadonia, J.W. Erning, U. Stimming, Proton cinduction of Nafion®-117 membrane between 140 K and room temperature, J. Electroanal. Chem. 376 (1994) 189–193.
[67] R.S. Yeo, Ion clustering and proton transport in Nafion membranes and its applications as solid polymer electrolyte, J. Electrochem. Soc. 130 (1983) 533–538.
[68] J.P. Meyers, J. Newman, Simulation of the direct methanol fuel cell-I. Thermodynamic framework for a multicomponent membrane, J. Electrochem. Soc. 149 (2002) A710–A717.